

Available online at [www.sciencedirect.com](http://www.sciencedirect.com)

Energy Procedia 1 (2009) 2969–2974

**Energy  
Procedia**[www.elsevier.com/locate/procedia](http://www.elsevier.com/locate/procedia)

GHGT-9

## Characterization of CO<sub>2</sub> storage properties using core analysis techniques and thin section data

Michael Krause<sup>a,\*</sup>, Jean-Christophe Perrin<sup>a</sup>, Chia-Wei Kuo<sup>a</sup>, and Sally M. Benson<sup>a</sup><sup>a</sup> *Stanford University, 367 Panama St, Stanford, CA 94305, USA*

---

### Abstract

Carbon dioxide capture and sequestration in saline aquifers is considered one of the most important technologies for short and medium term climate change mitigation. There are many challenges for wide scale deployment of sequestration, including developing a sufficiently accurate fundamental understanding of the processes which govern the movement of supercritical CO<sub>2</sub> in saline aquifers. A method for testing our understanding of the underlying physics is to conduct numerical simulations intended to replicate a multiphase flow experiment in which CO<sub>2</sub> is injected into a brine saturated rock core. This paper focuses on methods to integrate pore scale rock properties into permeability models of cores subjected to such experiments. We use thin sections to measure pore scale features of rocks, and test correlations that relate permeability to porosity using the Carman-Kozeny equation. Incorporation of these pore scale features into sub-core scale maps of permeability is being used to history match core-scale multi-phase flow experiments.

© 2009 Elsevier Ltd. Open access under [CC BY-NC-ND license](https://creativecommons.org/licenses/by-nc-nd/4.0/).

*Keywords:* CO<sub>2</sub> Storage; Sequestration; Saline Aquifers; Core Analysis; Thin Section Analysis; Permeability; Specific Surface Area, Carman-Kozeny

---

### 1. Introduction

The climate change problem requires a very broad range of solutions across many technologies and sectors, each with its own inherent set of opportunities and challenges. One of the most promising concepts is the sequestration of CO<sub>2</sub> in saline aquifers, which are estimated to have worldwide capacity up to 10,000 GtCO<sub>2</sub> [1]. In order to optimize the use of such capacity, it is important to understand in detail, the physics which govern the flow of fluids in the subsurface. A great deal of research on multiphase flows has been done for other applications (e.g. petroleum production, soil sciences, and vadose zone remediation), but fundamental research on the CO<sub>2</sub>-brine system is sparse and simple extension of existing principles needs to be examined and demonstrated.

With a facility for conducting CO<sub>2</sub>-brine multiphase flow experiments, we have the ability to test our understanding of the governing principles in multiphase flow for these systems by comparing and history matching experimental data using numerical simulation [2]. These experiments are conducted by injecting CO<sub>2</sub> and brine into a rock core until steady state is achieved, that is, until the saturation of CO<sub>2</sub> is no longer changing spatially or temporally [2]. Once this is done, a CT scan of the rock core can be made to map the spatial saturation of the CO<sub>2</sub> throughout the core during the experiment, as is shown below in Figure 1.

---

\* Corresponding author. Tel.: +1-650-725-0742 ; fax: +1-650-725-2099 .  
E-mail address: [krausm2@stanford.edu](mailto:krausm2@stanford.edu).

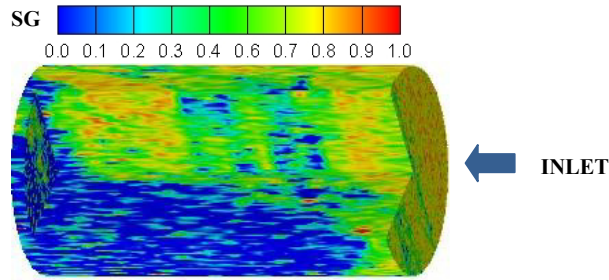


Figure 1. Saturation of supercritical CO<sub>2</sub> in a Berea sandstone core at steady state for 100% CO<sub>2</sub> injection

We then simulate these experiments using fundamental multiphase flow and thermodynamic principals, with the goal of replicating what is observed during the experiment. The degree to which we are successful is a measure of how well our current models predict multi-phase flow in CO<sub>2</sub>/brine systems. However, this is only true if we have accurate sub-core scale maps of the distribution of porosity, permeability and capillary pressure curves as input parameters for the simulations [3].

**2. Motivation**

When conducting experiments on a rock core, the spatial distribution of porosity is the most easily measurable parameter through the use of CT scanning, which can provide sub millimeter scale measurements of porosity. Other parameters previously mentioned, permeability and capillary pressure, must also be determined at the same scale in order to conduct simulations, however no method exists for easily measuring these values within a core at this scale. Therefore, determination of these parameters must be made using correlations to porosity.

Traditionally, porosity-based permeability estimates are determined using the Carman-Kozeny equation, which can include parameters such as porosity, tortuosity, specific surface area and average grain diameter. It can be expressed in a number of different forms, one common form is written as shown in Eq. 1.

$$k = \frac{c_o}{\tau \cdot a_v^2} \frac{\phi^3}{(1 - \phi)^2} \tag{1}$$

where k is permeability (m<sup>2</sup>), τ is the tortuosity (ratio of tortuous path length to straight path length), φ is porosity, a<sub>v</sub> is specific surface area (surface area of the pores per unit grain volume), and c<sub>o</sub> is Kozeny’s constant. In practice, because all of these parameters are difficult to measure except for porosity, the remaining parameters are typically combined into one constant to arrive at the form of the equation shown below in Eq. 2.

$$k = \frac{1}{S} \frac{\phi^3}{(1 - \phi)^2} \tag{2}$$

where S is called the shape factor. To determine capillary pressure, the Leverett J-function is used, shown in Eq. 3 below.

$$P_c = \sigma \cos(\theta) \sqrt{\frac{\phi}{k}} J(S_{nw}) \tag{3}$$

where σ is the interfacial tension (Pa-m), θ is the contact angle and J is the Leverett J-Function for the core.

From these relationships, permeability and capillary pressure can be derived from the porosity information collected by the CT scanner. Simulations conducted in prior work used Eq. 2 and 3 to the calculate permeability and capillary pressure. The simulations conducted using this approach have not been able to adequately match observed saturation distributions [3]. Therefore, this effort has focused on developing a better model for calculating permeability from porosity.

**3. Approach and Theoretical Background**

The approach taken here to improve the relationship is to use thin sections, which are transparent sections of rocks taken from the core, to provide more detailed information about the size and shapes of the pore spaces in the rock. By combining the information obtained from the thin sections with the porosity maps measured on the X-Ray CT Scanner, we seek to develop a better permeability map for the core.

Kozeny derived a relationship for permeability based on a capillary tube model whereby all tubes are the same length and have the same hydraulic radius. This relationship showed that permeability is a function of porosity and the amount of surface area of the pores per unit volume, as shown in Eq. 4 [4].

$$k = \frac{c_o \phi^3}{a_v^2} \tag{4}$$

where c<sub>o</sub> is Kozeny’s constant, φ is porosity and a<sub>v</sub> is specific surface area, or the surface area per unit volume of porous media. If we write this in terms of surface area per unit volume of solid, rather than porous media, the form of the Carman-Kozeny equation which we use is found and shown below in Eq. 5 [4].

$$k = \frac{c_o \phi^3}{a_v^2 (1 - \phi)^2} \quad 5$$

The average permeability of the core can be measured by injecting fluid at a constant flow rate and measuring the pressure drop across the core using Eq. 6.

$$q = \frac{kA P_1 - P_2}{\mu L} \quad 6$$

where  $q$  is the flow rate,  $A$  is the cross sectional area of the core,  $\mu$  is the fluid viscosity  $P_1$  and  $P_2$  are the inlet and outlet pressures respectively and  $L$  is the core length.

Specific surface area,  $a_v$ , can be determined from thin sections by measuring the perimeter of the pores and assuming that the three dimensional specific surface area is proportional to the two dimensional perimeter [5]. For a capillary tube bundle model, the specific perimeter is directly proportional to the specific surface area, and thus the derivation is consistent with this assumption. Porosity can also be measured from a thin section by calculating the area of the pores. Since the thin section comes from the same host rock as the core, we assume that the core and thin section have the same average permeability, therefore the value of Kozeny's constant  $c_o$  can be calculated using Eq. 5.

Together these measurements can be used as a basis for determining the spatial distribution of permeability and capillary pressure characteristic curves throughout the core using the method described below.

#### 4. Description of Method to Measure Specific Surface Area

A thin section is made by attaching a rock sample to a glass slide and grinding it down to 30  $\mu\text{m}$  thickness, at which point most rock minerals are transparent. A digital scan is then taken of the thin section using either a high resolution scanner or a custom scanning device. We use a 2400 dpi commercial scanner to get an image which can be analyzed using image processing software. A computer program has been written to convert the color image of the thin section to a grayscale image. Each pixel in the grayscale image has a value from 0 to 255, where 0 is black and 255 is white, in thin sections, white typically represents rocks because they are transparent. The image must be converted to binary (black and white) for processing, so a threshold value between 0 and 255 is selected such that everything above is converted to rock (black) and everything below is converted to pore space (white). This threshold value is selected such that the average porosity of the thin section is then the same as the average porosity of the core from which the thin section was made. The image conversion process is shown below in Figure 2.

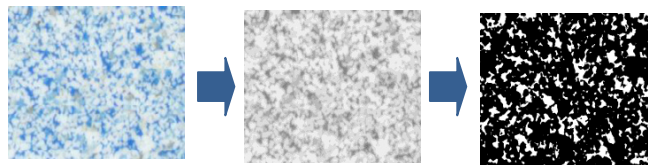


Figure 2. Thin section image conversion process, color image (left) is converted to grayscale (center) which is converted to binary (right) such that the average porosity of the binary image matches the measured average porosity of the core

This binary image of the thin section is then subdivided into regions of interest (ROI). The properties of each ROI are then analyzed and recorded. Recorded properties of each ROI include the total length of all of the perimeters of the pores, grain area fraction, and porosity. Figure 3 shows a sample ROI, the left image shows the grain (black) and porous areas (white) of a Berea sandstone (Berea 1), and the right image shows the outlines of the same pores which is used to calculate the perimeter in the ROI.

A thin section can be divided up into ROI's of any size; the number of data points is dependent upon the size, because each ROI in the thin section is one data point. For this study, the ROI was taken to be the same size as the long side of a single voxel from the X-Ray CT Scanner, 0.3 mm x 3 mm. For reference, the size of the images in Figure 3 was selected to show more detail than can be seen in a smaller ROI.

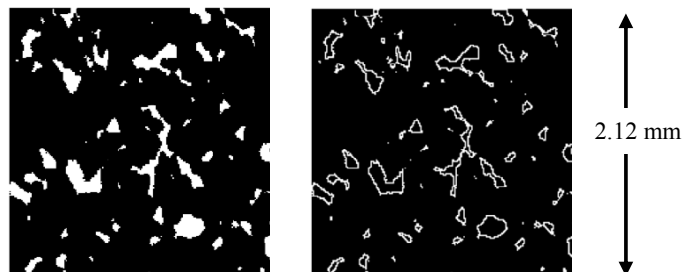


Figure 3: Map of an ROI from a thin section (left) showing porosity (white) and rock grain (black) and the subsequent trace of each pore (right)

With all of the thin section partitioned into ROIs and each ROI evaluated, a plot of the data can be prepared, with the specific perimeter of each ROI plotted against the porosity of each corresponding ROI, from this, a relationship correlating the specific perimeter to porosity is determined. The plot of the specific perimeter vs. the porosity for Berea 1 is shown below in Figure 4, which shows a power law trend.

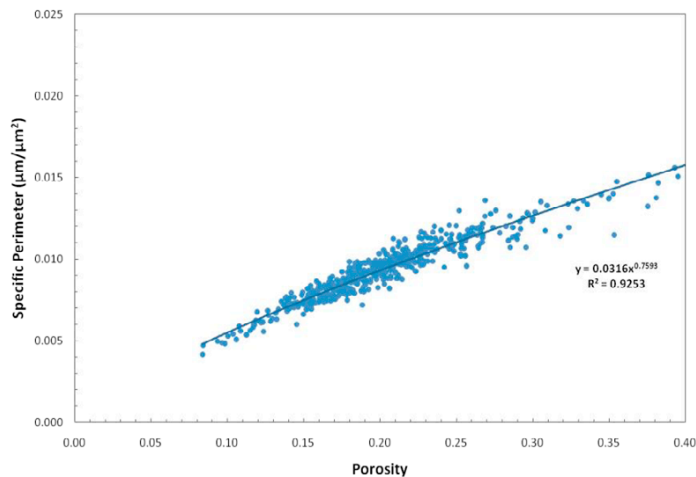


Figure 4. Specific perimeter vs. porosity for Berea 1

## 5. Permeability Results

Taking the regression line determined from Figure 4, Eq. 5 can be re-written to the form shown below in Eq. 7. From this, the porosity map of the dry core from the CT scanner can be used to create a permeability map. These maps are then used as input for numerical simulation.

$$k = \frac{c_o}{(0.0316\phi^{0.7593})^2} \phi^3 \quad 7$$

Using this relationship, a new permeability map was generated to simulate the experiment. For comparison, the permeability map using the original Carman-Kozeny equation (2) is shown below next to the permeability map using the modified Carman-Kozeny Eq. 7 in Figure 5.

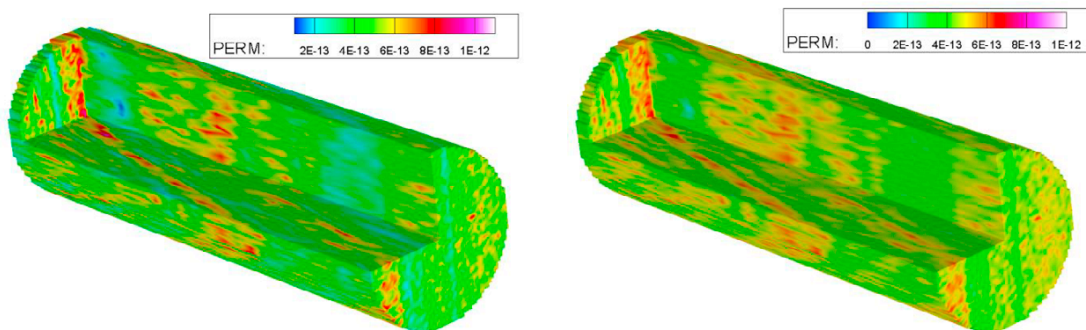


Figure 5. Permeability maps of Berea 1 using the original (left) and modified (right) Carman-Kozeny equation

From Figure 5 it is easy to see that the contrast between the regions of high and low permeability has decreased, which is an inevitable result of the form of the equation for specific perimeter. The trend in Figure 4 is not unique to Berea 1, indeed, two other samples were analyzed, one more Berea sandstone, called Berea 2, and another sandstone sample from the Waare C reservoir in the Otway Basin in Victoria, Australia. The results from the analysis on these thin sections are shown in Figure 6 below.

The results in the figure confirm the trend for specific perimeter as being repeatable across different cores, although the magnitude of the relationship between specific perimeter and porosity may change, the qualitative nature of it does not.

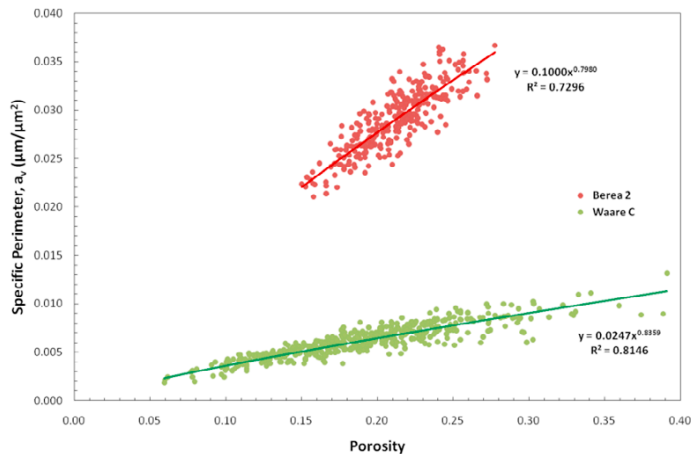


Figure 6. Specific Perimeter for Berea 2 and Waare C Rock Cores

## 6. Simulation of the Effects of Different Permeability Distributions on Saturation

The permeability and porosity information was input into the simulator and a simulation injecting a mixture of 50% CO<sub>2</sub> and 50% brine into a brine saturated core was conducted. The multi-processor version of TOUGH2 using the ECO2N module was used to conduct the simulations [3]. The saturation of supercritical CO<sub>2</sub> in the simulation is shown below in Figure 7. In the figure, the left image corresponding to permeability input calculated using the original method in Eq. 2 and the right image corresponding to permeability input calculated using the modified method in Eq. 7. The figure shows that the contrast in saturation between the high and low saturation regions has decreased when permeability is calculated using the modified method.

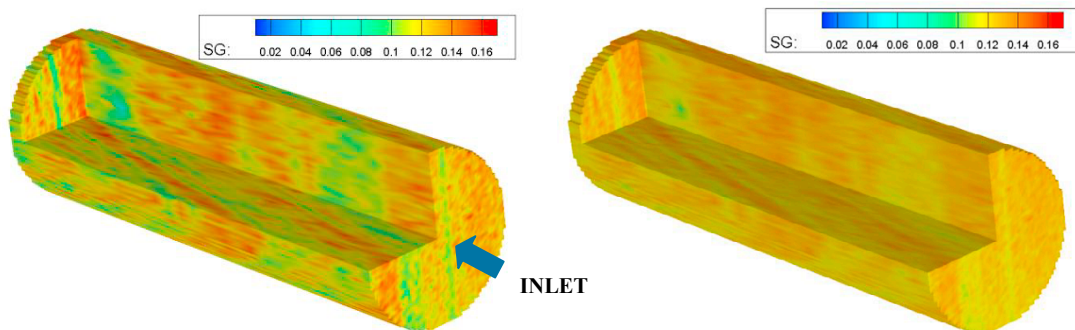


Figure 7. Saturation maps of Berea 1 using the original (left) and modified (right) Carman-Kozeny equation for 50% CO<sub>2</sub> injection.

When comparing Figure 5 with Figure 7, the regions of low saturation correspond to regions of low porosity and vice versa. This shows that changes in permeability will result in corresponding changes in saturation, in this case, a smoother permeability distribution results in a smoother saturation distribution throughout the core. This correlation can best be seen near the inlet face, where the low permeability streaks in the core shown in blue in Figure 5, produce corresponding low gas saturation in the same spatial location in Figure 7. The left and the right images both show similar gas saturation distributions, however, the left image shows more contrast than the image on the right.

As indicated in Eq. 3, permeability is also used to calculate the capillary pressure curves, leading to even greater importance in the outcome of history matching simulations. Consequently, history matching of core-scale displacements to test our ability to predict or validate simulation models will require accurate methods for estimating permeability distributions and capillary pressure curves. Given that porosity is the only rock property that can be directly measured using the X-ray CT scanner, a reliable method for extrapolating permeability from porosity is needed.

## 7. Conclusion

History matching core-scale multiphase flow experiments provides a unique means of testing our fundamental understanding and simulation methods for CO<sub>2</sub> sequestration in saline aquifers. Simulations show that saturation distribution in the core depends strongly on the permeability and thus the capillary pressure curves. Therefore, history matching will require accurate sub-core-scale maps of permeability and capillary pressure curves. This paper presents a new method for calculating permeability from porosity, based on extrapolating pore scale features (specific perimeter), measured from thin-sections, to the

core-scale. For the rocks evaluated here, the relationship between specific perimeter and porosity in a rock shows a distinct power law trend. This provides a simple method for modifying the traditional Carman-Kozeny relationship to account for rock-specific attributes.

Future work on this method for calculating permeability will continue along a number of paths: evaluating different rock types; by examining the effects of heterogeneity in more detail; and performing quantitative history matches with the experiments. In summary, the work presented provides a step in ongoing investigations into the pore and core scale phenomena of the CO<sub>2</sub> – brine system. This work provides insight into the important mechanisms in multiphase flow, and helps identify areas of research which require additional fundamental investigation.

## 8. Acknowledgements

The authors would like to gratefully acknowledge the generous support of the Global Climate and Energy Project (GCEP) for funding this research.

## 9. References

1. Intergovernmental Panel on Climate Change Report on Carbon Dioxide Capture and Storage, 2005, Cambridge University Press, New York, NY
2. J.C. Perrin and S.M. Benson. Core-scale experimental study of relative permeability properties of CO<sub>2</sub> and brine in reservoir rocks, Energy Procedia, Proceedings of the 9<sup>th</sup> International Conference on Greenhouse Gas Control Technologies (GHGT9), IEA Greenhouse Gas Programme, Washington D.C. USA, November 17-20, 2008.
3. L. Miljkovic, L. Tomutsa, C. Doughty, S.M. Benson. Observations of subcore-scale variability during multiphase flow of CO<sub>2</sub> and brine. Energy Procedia, Proceedings of the 9<sup>th</sup> International Conference on Greenhouse Gas Control Technologies (GHGT9), IEA Greenhouse Gas Programme, Washington D.C. USA, November 17-20, 2008.
4. J. Bear, Dynamics of Fluids in Porous Media, 1988, Dover Publications, Inc., Mineola, NY
5. C. Ross, pers. comm. 3 October, 2008.